Soft Matter

Accepted Manuscript

ROYAL SOCIETY OF CHEMISTRY

www.rsc.org/softmatter

Journal Name

ARTICLE

Unusual triskelion patterns and dye-labelled GUVs: Consequences of the interaction of cholesterol-containing linear-hyperbranched block copolymers with phospholipids

Received 00th January 20xx,
Accepted 00th January 20xx

DOI: 10.1039/x0xx00000x

www.rsc.org/

Peggy Scholtysek[a], Syed W. H. Shah[a], Sophie S. Müller[b,c], Regina Schöps[a], Holger Frey[b], Alfred Blume[a]* and Jörg Kressler[a]*

Cholesterol (Ch) linked to a linear-hyperbranched block copolymer composed of poly(ethylene glycol) (PEG) and poly(glycerol) (*hb*PG) was investigated for its membrane anchoring properties. Two polyether-based linear-hyperbranched block copolymers with and without covalently attached rhodamine fluorescence label (Rho) were employed (Ch-PEG_{30}-*b*-*hb*PG_{23} and Ch-PEG_{30}-*b*-*hb*PG_{17}-Rho). Compression isotherms of co-spread 1,2-dipalmitoyl-*sn*-glycero-3-phosphocholine (DPPC) or 1-palmitoyl-2-oleoyl-*sn*-glycero-3-phosphocholine (POPC) with the respective polymers were measured on the Langmuir trough and the morphology development of the liquid-condensed (LC) domains was studied by epi-fluorescence microscopy. LC domains were strongly deformed due to the localization of the polymers at the domain interface, indicating a line activity for both block copolymers. Simultaneously, it was observed that the presence of the fluorescence label significantly influences the domain morphology, the rhodamine labelled polymer showing higher line activity. Adsorption isotherms of the polymers to the water surface or to monolayers of DPPC and 1,2-dioleoyl-*sn*-glycero-3-phosphocholine (DOPC), respectively, were collected. Again the rhodamine labelled polymer showed higher surface activity and a higher affinity for insertion into lipid monolayers, which was negligibly affected when the sub-phase was changed to aqueous sodium chloride solution or phosphate buffer. Calorimetric investigations in bulk confirmed the results found with tensiometry. Confocal laser scanning microscopy (CLSM) of giant unilamellar vesicles (GUVs) also confirmed the polymers' fast adsorption to and insertion into phospholipid membranes.

Introduction

Biological membranes contain a complex mixture of different lipids, in the case of eukaryotic cell membranes mainly phospholipids, but also other components, such as proteins, lipoproteins and cholesterol are present. Phospholipids consist of a hydrophilic head group, which is zwitterionic in the case of phosphatidylcholines, and a hydrophobic tail with two fatty acyl chains. Phospholipids self-organize into vesicular bilayer systems in aqueous suspensions mimicking simplified cell membranes. In these liposomes the fatty acid chains form a hydrophobic membrane region, which is protected by the hydrophilic head groups from the outer and inner water phase of the vesicle. Phosphatidylcholines are of wide-spread occurrence in biological membranes and are commonly used as membrane models.[1-4]

Cholesterol is one of the most abundant molecules in biological membranes (4 to 50 mol%). It is a weakly amphiphilic molecule consisting of a hydrophobic sterol skeletal structure with a short branched alkyl chain and a hydrophilic hydroxyl group at the ring system. It appears in high amounts in eukaryotic cells and lipid domains,[1,5] for instance, in human erythrocyte plasma membranes as well as in almost all mammalian membranes.[6] Mixed lipid/cholesterol membranes have therefore been the subject of intense scientific research. Cholesterol incorporation into lipid bilayers enhances the membrane rigidity and stability.[7,8] Besides its behaviour in bilayer membranes,[6,9,10] also lipid/cholesterol monolayer systems have been studied in detail.[8,11-13] At the air/water interface, phospholipid monolayers undergo changes from a gaseous to a liquid expanded (LE) phase at large molecular areas. In the case of long chain saturated lipids, a phase transition into a liquid condensed (LC) state occurs upon further compression before the monolayer collapses at a high surface pressure. Furthermore, the LE/LC transition has much in common with the liquid-crystalline to gel phase transition in

[a] *Institute of Chemistry, Martin Luther University Halle-Wittenberg, von-Danckelmann-Platz 4, D-06120 Halle (Saale), Germany*
[b] *Institute of Organic Chemistry, Johannes Gutenberg University Mainz, Duesbergweg 10-14, D-55128 Mainz, Germany*
[c] *Graduate School Materials Science in Mainz, Staudingerweg 9, D-55128 Mainz, Germany*

† Footnotes relating to the title and/or authors should appear here.
Electronic Supplementary Information (ESI) available: [details of any supplementary information available should be included here]. See DOI: 10.1039/x0xx00000x

bilayer systems. Earlier calorimetric studies of the effect of cholesterol on the first order phase transition of phospholipids have shown that with increasing cholesterol concentration the temperature of the main LE/LC transition is gradually broadened and no phase transition is observed above a concentration of 50 mol% cholesterol, where in many cases cholesterol separates out of the membrane.[1,14,15] Cholesterol exhibits a so-called "condensing effect" on liquid-crystalline bilayers,[1,7,10] which can be understood as the induction of an intermediate state of the lipid acyl chains between the ordered and the liquid crystalline state. In this intermediate state, the acyl chains are in an all-trans conformation but the molecules can rotate freely around their long axis. In lipid monolayers at the air/water interface this condensing effect on the liquid-expanded phase can be directly observed by a reduction of the mean molecular area.[1,12]

Furthermore, cholesterol has been modified chemically for various applications in life sciences. Cholesteryl hemisuccinate is employed for mimicking cholesterol in phospholipid bilayers.[16] It stabilizes these bilayers[17] and it is frequently employed in studies on membrane protein crystallization.[18] The OH-group of cholesterol is perfectly suited for conjugation with polymer chains. The attachment of water soluble synthetic polymers is broadly used as e.g. poly(ethylene glycol) (PEG)[19] or biopolymers.[20] These amphiphilic polymers are then employed for stabilizing meso- and nanostructures as micelles, liposomes and polymersomes.[21] There is a large potential for applications in drug release systems in pharmacy and nanomedicine.[22,23]

In this study, we employ cholesterol as an anchor for inserting a non-natural linear-hyperbranched block copolymer into lipid monolayers and bilayers. Cholesterol is linked via its hydroxyl group to a linear poly(ethylene glycol) (PEG) block and a hyperbranched poly(glycerol) (*hb*PG) block (Scheme 1). Both polymer segments are hydrophilic in nature and known to be highly biocompatible.[28,29] The interaction of two block copolymers Ch-PEG$_{30}$-*b*-*hb*PG$_{23}$ and Ch-PEG$_{30}$-*b*-*hb*PG$_{17}$-Rho, where Rho stands for the covalently attached rhodamine fluorescence label (Scheme 1), with saturated and unsaturated phospholipids at the air/water interface and in lipid bilayers is investigated. 1,2-Dipalmitoyl-*sn*-glycero-3-phosphocholine (L-DPPC), 2,3-dipalmitoyl-*sn*-glycero-1-phosphocholine (D-DPPC), 1-palmitoyl-2-oleoyl-*sn*-glycero-3-phosphocholine (POPC), 1,2-dilauroyl-*sn*-glycero-3-phosphocholine (DLPC) and 1,2-dioleoyl-*sn*-glycero-3-phosphocholine (DOPC) are used as model lipids. The experiments are based on previous studies employing this type of linear-hyperbranched block copolymers.[24-26] Monolayer experiments were combined with epi-fluorescence microscopy, and interactions of the fluorescent labelled block copolymer with phospholipid bilayers were studied by confocal laser scanning microscopy (CLSM) employing giant unilamellar vesicles (GUVs).

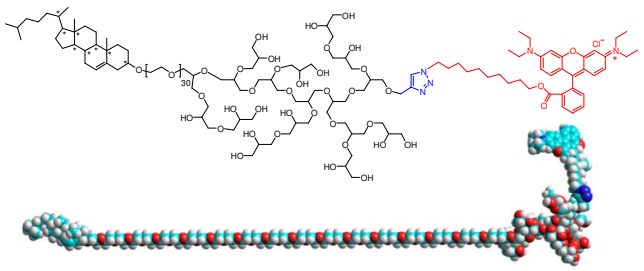

Scheme 1 Chemical structure of the rhodamine labelled Ch-PEG$_{30}$-*b*-*hb*PG$_{17}$-Rho and its CPK model with the PEG chain in an extended form.

Experimental

Materials

All reagents and solvents for syntheses were purchased from Acros Organics (Geel, Belgium) and used as received unless otherwise mentioned. Dry solvents were stored over molecular sieves. DMSO-d_6 was purchased from Deutero GmbH (Kastellaun, Germany). Ethoxyethyl glycidyl ether (EEGE) was synthesized as described before[27] and dried over CaH_2 prior to use. Glycidol was purified by distillation from CaH_2 directly prior to use.

1,2-Dipalmitoyl-*sn*-glycero-3-phosphocholine (L-DPPC) and 2,3-dipalmitoyl-*sn*-glycero-1-phosphocholine (D-DPPC) were purchased from Sigma Aldrich (Schnelldorf, Germany) with purity > 99 %. 1-Palmitoyl-2-oleoyl-*sn*-glycero-3-phosphocholine (POPC), 1,2-dilauroyl-*sn*-glycero-3-phosphocholine (DLPC), 1,2-dioleoyl-*sn*-glycero-3-phosphocholine (DOPC) and 1-palmitoyl-2-oleoyl-*sn*-glycero-3-phosphoglycerol (POPG) were purchased from Genzyme Pharmaceuticals (Liestal, Switzerland) with purity > 99 %. The head group-labelled fluorescence dye 1,2-dihexadecanoyl-*sn*-glycero-3-phosphoethanolamine-*N*-(lissaminerhodamine B sulfonyl) (Rhodamine-DHPE), the fatty acid labelled fluorescence lipid 1-acyl-2-{12-[(7-nitro-2-1,3-benzoxadiazol-4-yl)amino]dodecanoyl}-*sn*-glycero-3-phosphocholine (NBD C_{12}-HPC) as well as the carbocyanine dye DiO were purchased from Invitrogen (Karlsruhe, Germany). 1,2-Distearoyl-*sn*-glycero-3-phosphoethanolamine-N-[biotinyl(polyethylene glycol)-2000] ammonium salt (DSPE-PEG-Biotin) with purity > 99 % was purchased from Avanti Polar Lipids (Alabaster, AL, USA). Streptavidin, bovine serum albumin (BSA) and biotinylated BSA were purchased from Sigma Aldrich (Schnelldorf, Germany) and used for glass coating in confocal microscopy experiments. Physico-chemical analyses and sample preparation were performed with ultrapure water from Millipore Quality (conductivity < 0.055 µS/cm, total organic carbon (TOC) < 5 ppm). Organic solvents for sample preparation were of HPLC-grade purity.

Synthesis of Ch-PEG$_{30}$-*b*-*hb*PG$_{23}$ and Ch-PEG$_{30}$-*b*-*hb*PG$_{17}$-Rho

The protocol was slightly modified from previous literature[28,29] and therefore the detailed procedure is given here. For the synthesis of the non-labelled polymer, cholesterol (1.38 g, 3.6

mmol), CsOH monohydrate (0.539 g, 3.2 mmol; resulting in a degree of deprotonation of cholesterol of 90 %), and benzene were placed in a Schlenk flask. The mixture was stirred for about 30 min to generate the deprotonated species. The formed salt was dried under vacuum at 90 °C for 24 h, anhydrous tetrahydrofuran (THF) was added via cryo transfer, and ethylene oxide (5 mL, 100 mmol) was cryo transferred first to a graduated ampule and then to the Schlenk flask containing the initiator solution. The mixture was allowed to warm up to room temperature, heated to 60 °C, and the polymerization was performed for 12 h at 60 °C in vacuum. Subsequently, a sample was removed for NMR and SEC analyses. Ethoxyethylglycidyl ether (EEGE) (3.8 mL, 25 mmol) was injected with a syringe, and the reaction mixture was held at 60 °C for additional 12 h. After removal of another sample for characterization, the polymerization was stopped with an excess of methanol and acetal protecting groups of the PEEGE block were removed by addition of water and acidic ion-exchange resin, stirring for 12 h at 40 °C. The solution was filtered, concentrated, and the crude product was precipitated in cold diethyl ether. The block copolymer was dried in vacuum. Yield ~90%. Size exclusion chromatography (SEC): M_n= 1100 g mol^{-1}, PDI= 1.16. NMR: M_n= 3600 g mol^{-1}.

For synthesis of the labelled polymer the same macroinitiator Ch-PEG$_{30}$ was employed. For hypergrafting of the *hb*PG-block, the macroinitiator was placed in a Schlenk flask suspended in benzene, CsOH monohydrate was added to achieve 25 % of deprotonation of the total amount of hydroxyl groups and after 30 min the mixture was dried under vacuum. The macroinitiator was dissolved in diethylene glycol dimethyl ether (diglyme) (25 wt %), heated to 90 °C and a 25 wt% solution of glycidol in diglyme was added slowly with a syringe pump over a period of 18 h. Termination was carried out with an excess of methanol and an acidic ion exchange resin. The crude product was filtrated, precipitated in cold diethyl ether and the Ch-PEG-*b*-*hb*PG block copolymer was dried in vacuum. Yield ~80%. SEC: M_n= 1170 g mol^{-1}, PDI= 1.27, NMR: M_n= 3430 g mol^{-1}. The rhodamine-B-11-azido-undecanyl ester was attached to the alkyne-functionalized polymer by click reaction (see ESI†, Scheme S1; NMR for alkyne-functionalized polymer see Fig. S2). The procedures were carried out as described elsewhere.[29,33]

Polymer characterization

^{1}H NMR spectra were recorded using a Bruker AC 300 spectrometer operated at 300 MHz, employing DMSO-d_6 as solvent. SEC measurements were carried out in dimethylformamide (DMF) with 0.25 g L^{-1} LiBr. For SEC measurements a UV (275 nm) and an RI detector were used. Calibration was carried out using poly(ethylene glycol) standards provided by Polymer Standards Service (PSS, Mainz, Germany).

Langmuir compression isotherms

The monolayer isotherms of mixed and pure DPPC and both polymers were determined using a Langmuir film balance (Riegler & Kirstein GmbH, Berlin, Germany; total area of 536 cm^2) with a compression ratio of 11.5. Pure and mixed samples were prepared from organic stock solutions to a total concentration of 1 mM in a solvent mixture of 9:1 (v:v) chloroform:methanol. After spreading the required amount of sample solution to the surface the solvent was allowed to evaporate for at least 10 min. Continuous compression of the monolayers was performed with a constant compression rate of 2 Å^2 molecule^{-1} min^{-1} until the collapse pressure of the respective monolayers was reached. For recording the isotherm of pure lipid and mixed lipid/polymer samples only one compression run was needed to cover the complete area range for all phases. For pure polymers the compression isotherms had to be combined from two measurements, respectively, due to their high area requirements. Measurements were performed at 20 °C.

Epi-fluorescence microscopy

The experimental setup for epi-fluorescence microscopy consisted of an upright epi-fluorescence microscope Axio Scope A1 Vario (Carl Zeiss MicroImaging, Jena, Germany) with an HXP 120 C lamp and a Langmuir film balance (Riegler & Kirstein GmbH, Berlin, Germany; area of 264 cm^2). The film balance was mounted on an x-y-stage (Märzhäuser, Wetzlar, Germany; x-y-z-motion control by Mac5000, Ludl Electronic Products, Hawthorne, USA).

Pure lipid samples were prepared at a concentration of 1 mM in chloroform, mixed samples of lipid and polymer in different molar ratios 100:1 to 5:1 and pure polymer solutions were prepared to a total concentration of 1 mM each in a 9:1 (v:v) solvent mixture of chloroform:methanol. After spreading the samples, the solvent was allowed to evaporate for at least 10 min. Measurements were performed at 20 °C. As fluorescence dye the head group labelled lipid rhodamine-DHPE ($\lambda_{ex/em}$ = 557/571 nm) was added in an amount of only 0.01 mol%. The electron multiplier effect of the 3 CCD camera (ImageEM C9100-13, Hamamatsu, Herrsching, Germany) allowed the use of these very low fluorescence label concentrations. The isotherms of the lipid-polymer mixtures were thus not influenced by the added fluorescence label. The Zeiss filter set 20 (green light) was used for fluorescence excitation of rhodamine-DHPE alone. Filter set 58 HE was used for co-localisation experiments with the rhodamine-labelled polymer Ch-PEG$_{30}$-*b*-*hb*PG$_{17}$-Rho co-spread with DPPC. The used objective was a long distance LD EC Epiplan-NEOFLUAR with 50x magnification to observe the lipid domain formation at the air/water interface. Fluorescence images were taken during constant compression of the monolayers with a compression rate of 2 Å^2 molecule^{-1} min^{-1}. The images were collected with the Zeiss AxioVision software (Carl Zeiss MicroImaging, Jena, Germany).

Adsorption measurements at the air/water interface

Adsorption studies of the polymers were performed with a home-built circular film balance with fixed surface area of 28.3 cm^2 and a subphase volume of 8.48 mL. All measurements were performed at a temperature of 20 °C. . To achieve a homogeneous distribution of the injected polymers in the subphase a small stainless steel ball moving slowly in the field of a magnetic stirrer positioned underneath the trough was

used as a stirrer. For surface activity tests aqueous solutions of the polymers with concentrations lower than the critical aggregation concentration (cac) were injected underneath the water surface to reach defined polymer concentrations from 500 nM up to 9 µM. For adsorption studies of the polymers to lipid monolayers, the lipid was first spread to different initial lateral surface pressures. Injections of the polymer solutions were then carried out 30 min after formation of the phospholipid monolayers. Measurements of the surface pressure were performed after the injection up to 20 h. The measurements were repeated using aqueous sodium chloride solution (100 mM) and phosphate buffer (pH 7.0) as sub-phases.

Differential scanning calorimetry (DSC)

Calorimetric investigations were performed with a VP-DSC microcalorimeter (MicroCal Inc., Northhampton, USA). Pure or mixed aqueous samples were prepared following the thin film preparation method[30] using higher concentrated stock solutions in organic solvents. After adding water to the lipid films to reach a total concentration of 2 mM the samples were vortexed several times at about 67 °C and afterwards cooled to room temperature and filled into the sample cell of the DSC instrument. The reference cell was filled with ultrapure degassed water. Consecutive scans in a temperature range of 5-60 °C were performed to test for reproducibility. The water-water baseline was subtracted from the sample thermograms before analysis, using the software ORIGIN (MicroCal Inc., Northhampton, USA). The thermograms presented in the figures are always from the fourth heating scan.

Confocal laser scanning microscopy (CLSM)

GUVs were prepared from a thin dried film of 10 nmol phospholipid after addition of 570 µL deionized water. A modified variant of electroformation,[31] using a chamber, constructed from two ITO coated glass slides with a silicon ring seal in between, connected to a frequency generator was used. A frequency of 10 Hz and a voltage of 3 V was used for the alternating electrical field applied to the sample held at a temperature of 60 °C. The phosphocholines (DLPC, POPC, DOPC) were mixed with 2 mol% POPG to avoid GUV aggregation. The GUVs were immobilized on a streptavidin coated glass surface using 0.3 mol% DSPE-PEG-Biotin to the lipids. For visualization 0.1 mol% DiO ($\lambda_{ex./em.}$ = 487/501 nm) was added as a fluorescent membrane dye.

A chamber of nearly 230 µL volume, formed by fixing a silicon ring (10 mm diameter, 3 mm high) onto a coverglass, passivated with BSA/biotinylated BSA in a molar ratio 10:1 and subsequently coated by streptavidin[32] was used for microscopic observation of the polymer adsorption. A 57 µL aliquot of freshly prepared GUV suspension (~1 nmol PC) was added to pure water in the chamber and GUVs were immobilized through the biotin containing phospholipid moiety onto the streptavidin coated cover glass surface. The actual amount of PC in the sample was controlled by comparing the overall intensity of the membrane dye emission against a phospholipid/DiO standard. Appropriate volumes of a 10 µM aqueous polymer solution were added stepwise to obtain molar polymer/PC ratios of 1/100 to 1/2. For long-lasting observations the chamber was sealed by a second coverslip on top to avoid evaporation. All experiments were carried out at room temperature.

A Leica TCS SP2 DM IRE2 confocal microscope was used with a HCX PL APO 63 x 1.4 oil immersion objective (Leica Microsystems, Wetzlar, Germany) for two channel imaging. GUV membranes with DiO as membrane dye were visualized by excitation at 488 nm, detecting the emission at 500-520 nm. The rhodamine labelled polymer was excited at 543 nm and detected at 610-630 nm to avoid cross-talk. For quantitative analysis of the adsorption intensity the emission in the equatorial slice of the GUV membrane was used. Single scans were analyzed with Leica Quantify Software using the regions of interest (ROI), as described elsewhere[33] and illustrated in the supporting information (ESI†, Fig. S3). Data shown are in agreement with the observation of a single GUV over time or with addition of increasing polymer ratios. Each experiment was repeated several times to guarantee reproducibility.

Results and discussion

Tensiometry and epi-fluorescence microscopy of monolayers

Monolayers can be interpreted as half of a membrane[34] and can be easily prepared and controlled. The properties of monolayers of phospholipids and cholesterol have been thoroughly investigated in the past. To understand how the newly synthesized polymers interact with lipid bilayers and monolayers, we determined first monolayer isotherms of Ch-PEG_{30}-*b*-*hb*PG_{23} and Ch-PEG_{30}-*b*-*hb*PG_{17}-Rho using a Langmuir trough in combination with epi-fluorescence microscopy to check for possible film heterogeneity (see Fig. 1). The polymers have much larger molecular areas due to their voluminous head groups (hydrophilic blocks) compared to lipids. Therefore the isotherms had to be "stitched" together from two separate compression experiments. The two pieces of the isotherms are plotted separately into one diagram in order to demonstrate the reproducibility. Both polymer monolayers can be compressed to high lateral surface pressures of 38.3 mN m^{-1} for Ch-PEG_{30}-*b*-*hb*PG_{23} and 33.1 mN m^{-1} for Ch-PEG_{30}-*b*-*hb*PG_{17}-Rho, respectively, before film collapse. The relatively high stability of the monolayer is due to the hydrophobic cholesterol unit anchoring the very hydrophilic polymers at the air/water interface. In both compression isotherms, a slight change in slope is observed at a surface pressure of around 7.4 mN m^{-1} (see arrows in Fig. 1a), indicating a squeeze-out of the hydrophilic PEG into the water subphase.[35,36] Further compression results in a transition at ~31 mN m^{-1} for Ch-PEG_{30}-*b*-*hb*PG_{23} and 22-25 mN m^{-1} for Ch-PEG_{30}-*b*-*hb*PG_{17}-Rho (see arrows in Fig. 1a). The kink found in the compression isotherm of the rhodamine labelled copolymer monolayer is reproducibly found at lower surface pressure when Ch-PEG_{30}-*b*-*hb*PG_{17}-Rho is spread to smaller initial areas per polymer molecule. The transition reflected by the kink found for both polymers is not related to the pronounced transition from the

gaseous state to the crystalline state found for pure cholesterol, because this occurs at much lower area per molecule (see Fig. 1d).[24,37] Instead it is caused by a structural rearrangement of the hydrophilic headgroups of the polymers consisting of the PEG spacer and the hyper-branched poly(glycerol) block. This rearrangement is well known from phospholipids with attached PEG chains. In DPPE-PEG2000 similar transitions are seen at surface pressures of 8 and 28 mN m^{-1}. The current interpretation of these transitions is the following: At high molecular area the PEG chain is located at the air-water interface and adopts the form of a pancake. Upon compression, a first transition into the so-called mushroom conformation occurs, where the PEG-chain is displaced from the air-water surface and extends into the subphase in mushroom-like conformation. At high pressure and lower molecular area the PEG-chain extends even more into the subphase forming the so-called brush conformation. The pressure and area at which these transitions occur depend on the number of EG units in the chain.[38-41] For our polymers with the cholesterol anchor a similar behaviour is obviously present, however, modified by the presence of the hydrophilic poly(glycerol) group. As can be seen from the CPK model (see Scheme 1) of Ch-PEG_{30}-*b*-*hb*PG_{23}, the PEG chain is dominant in the area requirement at lower surface pressure while at higher pressure and areas below 100 $Å^2$/molecule, when the PEG chain becomes more extended, the poly(glycerol) block will be the determining factor for the area occupied at the air-water surface.

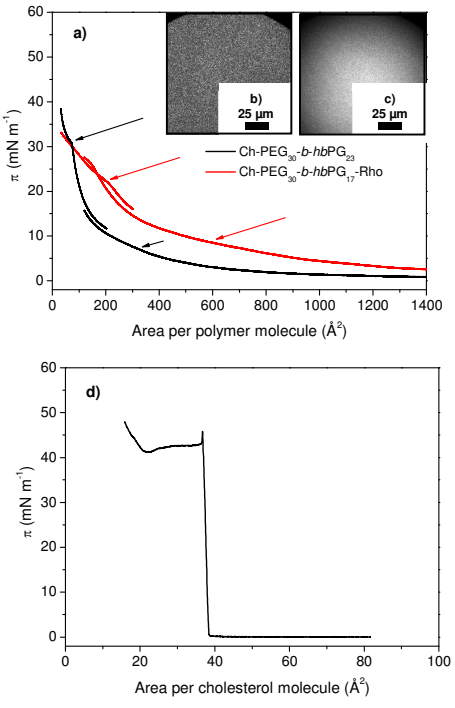

Fig. 1 a) Compression isotherms of pure polymer monolayers; inset b) epi-fluorescence microscopy image of Ch-PEG_{30}-*b*-*hb*PG_{23}, 32.3 mN m^{-1}; fluorescent dye: 0.01 mol% rhodamine-DHPE. For the meaning of the arrows see text. Inset c) epi-fluorescence microscopy image of Ch-PEG_{30}-*b*-*hb*PG_{17}-Rho, 32.2 mN m^{-1}; d) compression isotherm of pure cholesterol.

In order to investigate the influence of Ch-PEG_{30}-*b*-*hb*PG_{23} and Ch-PEG_{30}-*b*-*hb*PG_{17}-Rho on the monolayer isotherms of different phosphatidylcholines, samples with molar mixing ratios from 100:1 to 5:1 phospholipid:polymer were co-spread to form mixed monolayers at the air/water interface and then compressed on the Langmuir trough (see Fig. 2). The influence of both polymers on the observed isotherms is similar when mixed with L-DPPC or POPC. The lift-off of the mixed monolayer isotherms changes from a sharp rise at definite areas per lipid molecule, e.g. 85 $Å^2$ $molecule^{-1}$ for L-DPPC, to a broader range for the molecular area when mixed monolayer are compressed. As expected, the lift-off shifts to higher areas per lipid molecule the higher the amount of polymer in the mixture. For instance, for the mixture of L-DPPC:Ch-PEG_{30}-*b*-*hb*PG_{17}-Rho = 5:1, it is shifted to more than 400 $Å^2$ $molecule^{-1}$ (see Fig. 2c). The plateau region of the phase transition of L-DPPC is shifted to higher lateral pressures, e.g. from 5.2 mN m^{-1} for pure L-DPPC up to 10.8 mN m^{-1} for the mixture of L-DPPC:Ch-PEG_{30}-*b*-*hb*PG_{17}-Rho = 5:1, due to the polymer incorporation, indicating a destabilization of the LC phase. At higher polymer content, the pancake-mushroom transition of the polymer coincides with the LE-LC transition of DPPC. This is particularly evident when mixtures with DPPC are compared with those containing POPC, in which the LE-LC transition is absent (see Fig. 2a,b for Ch-PEG_{30}-*b*-*hb*PG_{23} and black arrows in Fig. 2c,d for Ch-PEG_{30}-*b*-*hb*PG_{17}-Rho). Upon further compression, the mushroom to brush transition of the polymer remains visible, particularly for the mixtures with Ch-PEG_{30}-*b*-*hb*PG_{17}-Rho it is quite pronounced and occurs at pressures of around 30-32 mN m^{-1} (see red arrows). The molecular area shown in Fig. 2 is calculated based on the phospholipid content. The shifts in molecular area are therefore mainly due to the presence of the polymer. At a surface pressure of 40 mN m^{-1} the molecular area of a 5:1 mixture of DPPC with Ch-PEG_{30}-*b*-*hb*PG_{23} (16.6 mol%) is 59 $Å^2$ per molecule of DPPC. The molecular area of pure cholesterol at this pressure is 38 $Å^2$ compared to pure DPPC with a molecular area of 48 $Å^2$. The observed difference of 10 $Å^2$ $molecule^{-1}$ of DPPC is thus larger than the calculated difference (7.6 $Å^2$ $molecule^{-1}$ of DPPC) with the assumption that only the cholesterol anchor contributes to the molecular area. The conclusion is that at this pressure the polymer is still stably inserted into the monolayer as the available space for the polymer head group (5 x 48 $Å^2$ (DPPC) + 38 $Å^2$ (cholesterol) ≈ 278 $Å^2$) is still large enough for its accommodation below the lipid head groups in the subphase. As can be seen in Fig. 1, the mushroom-brush transition for Ch-PEG_{30}-*b*-*hb*PG_{23} occurs below a molecular area of 100 $Å^2$ per polymer. The polymer head group in the mixture with DPPC can therefore adopt the mushroom conformation even at a surface pressure of 10 mN m^{-1}.

Similar results are obtained for mixtures with Ch-PEG_{30}-*b*-*hb*PG_{17}-Rho, though in this case the mushroom-brush transition occurs at higher molecular area. This is also evident in the isotherms of the mixtures where this occurs at a

molecular area of ~100 Å^2 per lipid for the 5:1 mixture (see Fig. 2c).

POPC is in the LE state at room temperature. Therefore, the pseudo-plateau for the LE-LC transition is missing in the isotherms (Fig. 2b,d) and only the transitions of the polymer remain visible, particularly the pancake to mushroom transition at lower surface pressure (see black arrow). The mushroom to brush transition is somewhat obscured due to the lower stability of the monolayers containing POPC. The collapse pressures of the mixed monolayers are hardly affected by the addition of the polymer and are in the range between 48 and 55 mN m^{-1} for mixtures with DPPC and between 42 and 44 mN m^{-1} for mixtures with POPC, which show again lower stability.

To obtain further information on morphological behaviour of the co-spread PC/polymer monolayers in the LE-LC transition region, epi-fluorescence microscopy images were recorded. Monolayers of the mixtures of L-/D- and rac-DPPC with both polymers with different mixing ratios were prepared and images were recorded at different surface pressures during constant compression of the film at a low compression rate. The images shown in Figures 3 and 4 were obtained for the mixtures of L- or rac-DPPC:Ch-PEG$_{30}$-*b*-*hb*PG$_{23/17}$(-Rho) = 10:1.

The observed domain shapes are quite different for both polymers in the mixture with L- and rac-DPPC, respectively. For monolayers of mixtures of L-DPPC:Ch-PEG$_{30}$-*b*-*hb*PG$_{23}$ = 10:1, thinned domains which still exhibit the typical triskelion domain shape as found for pure L-DPPC could be observed (Fig. 3a). Domain thinning results from the insertion of the cholesterol anchor of the amphiphilic block copolymer into the monolayer and its enhanced accumulation at the phase boundary of the LC lipid domains. The domain boundary of the LC-L-DPPC domain exhibits a lower line tension than without the polymer. This lower line tension allows for repulsive forces to dominate, leading to an elongation of the former compact triskelion domains.[42-44] Domain thinning has also been observed for mixtures of DPPC with pure cholesterol at a concentration of only 2 mol% cholesterol.[45] Differences in domain shapes observed here from the domain shapes of L-DPPC with co-spread pure cholesterol, result from the influence of the hydrophilic hyperbranched poly(glycerol) and the linear poly(ethylene glycol) blocks. As can be seen in Figure 3b, regular protuberances develop in the inside of the LC triskelion shaped domains, which can be related to the macromolecular crowding at the interface.

Upon further compression of the L-DPPC:Ch-PEG$_{30}$-*b*-*hb*PG$_{23}$ monolayer, growth of the LC domains occurs and the protuberances seem to be reduced (see Figure 3c). Protuberances only occur on the inside of the domain arms. Here, the line tension is lower than at the strongly curved outside. Within the LC domains and in places where repulsion dominates the line tension, the excrescences develop.

Totally different domain shapes result from the addition of the rhodamine labelled polymer Ch-PEG$_{30}$-*b*-*hb*PG$_{17}$-Rho to L-DPPC (see Fig. 3 d-f). A tremendous lowering of the line tension is observed, indicated by the formation of very narrow domain stripes, which are frequently curled. The stripes do not coalesce upon further compression of the monolayer; hence the driving force for reducing the domain length between LE and LC domains is very low. From a chemical point of view, the only differences between the two polymers Ch-PEG$_{30}$-*b*-*hb*PG$_{23}$ and Ch-PEG$_{30}$-*b*-*hb*PG$_{17}$-Rho are the number of six glycerol units in the hyperbranched region and the additional covalently linked rhodamine label. These structural differences are both located within the hydrophilic region of the polymer, which is located at the air-water interface at large molecular areas in the so-called pancake regime. At surface pressures between 10-14 mN m^{-1}, the polymer is already in the mushroom conformation and should be extended into the subphase. The observed striking differences in the monolayer behaviour of these two polymers indicate that for Ch-PEG$_{30}$-*b*-*hb*PG$_{17}$-Rho specific interactions between the hydrophilic head group of the polymer and the head groups of the phosphatidylcholine must exist. Most likely, additional hydrogen-bonding and hydrophobic interactions are

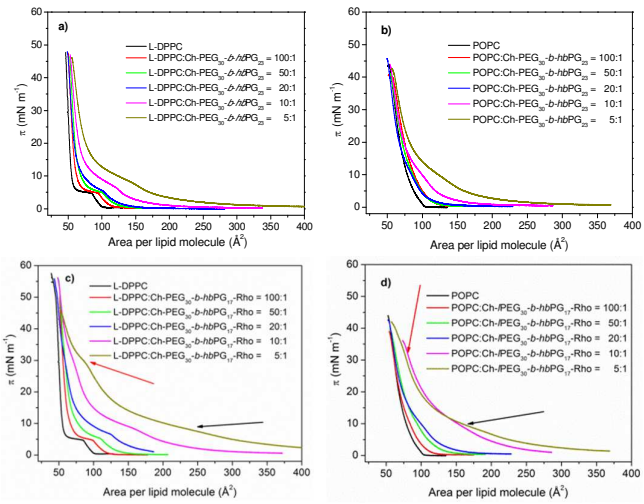

Fig. 2 Compression isotherms of co-spread mixtures of the phospholipids L-DPPC and POPC in the mixture with the polymers Ch-PEG$_{30}$-*b*-*hb*PG$_{23}$ and Ch-PEG$_{30}$-*b*-*hb*PG$_{17}$-Rho in molar ratios of 100:1 to 5:1 phospholipid:polymer. For the meaning of the arrows see text.

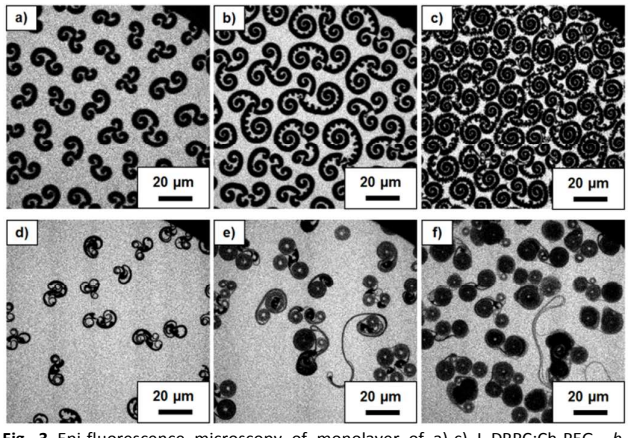

Fig. 3 Epi-fluorescence microscopy of monolayer of a)-c) L-DPPC:Ch-PEG$_{30}$-*b*-*hb*PG$_{23}$ = 10:1 and d)-f) L-DPPC:Ch-PEG$_{30}$-*b*-*hb*PG$_{17}$-Rho = 10:1 at surface pressures of a) 9.8 mN m^{-1}, b) 14.0 mN m^{-1}, c) 23.9 mN m^{-1}, d) 10.3 mN m^{-1}, e) 11.8 mN m^{-1}, f) 14.2 mN m^{-1}. Fluorescent dye: 0.01 mol% rhodamine-DHPE.

occurring. The fluorescent label is connected to the poly(glycerol) block via a hydrophobic spacer. The rhodamine moiety is composed of conjugated aromatic rings but also carries a positive charge. Therefore, this moiety is by itself amphipathic and may well be able to also insert into the interfacial region of the lipid head groups. The observed larger molecular areas in mixtures of PCs with Ch-PEG$_{30}$-*b*-*hb*PG$_{17}$-Rho support this proposition.

Likewise, the observed domain shapes indicate a much lower line tension between the domains caused by the additional interaction of the attached rhodamine dye with the lipid monolayer. For D-DPPC mixtures with the block copolymers very similar domain shapes are observed with the exception that the curling direction is opposite (images not shown).

The polymers with eight stereogenic centers within the cholesterol unit were investigated for their ability to influence the DPPC domain chirality at the air/water interface. For this purpose, the polymers were mixed and co-spread with a racemic mixture of L- and D-DPPC. Epi-fluorescence images of the mixed monolayers in the LE-LC coexistence region are shown in Fig. 4. Neither in mixtures of both polymers with L- or D-DPPC nor with racemic DPPC, we observed a change in domain chirality. The preferred curling direction of L- and D-DPPC triskelions, induced by their own stereogenic center in the hydrophilic head group and the 30° tilt of the fatty acid chains[46], is unaltered by the incorporation of the cholesterol containing polymers. For racemic DPPC condensed domains without a preferred curling direction were observed. At higher lateral compression, the LC domains appeared as bundles of parallel oriented stripes.

In monolayers of racemic DPPC the LC domains found for the mixture rac-DPPC:Ch-PEG$_{30}$-*b*-*hb*PG$_{23}$ 10:1 are again much thinner and thus affected by the cholesterol unit of the polymer and additionally by the hydrophilic blocks of poly(ethylene glycol) and hyperbranched poly(glycerol) (see Fig. 4 a-c). The observed domain thinning effects again result from a lower line tension compared to the original phase boundary between the two co-existing DPPC phases.[42-45] As already observed, the rhodamine labelled polymer Ch-PEG$_{30}$-*b*-*hb*PG$_{17}$-Rho has a totally different effect on the domain shapes compared to the polymer Ch-PEG$_{30}$-*b*-*hb*PG$_{23}$. The very thin striped domains start to grow from a star-like domain and run almost parallel over large distances. The stripe-like domains are very stable and do not coalesce upon compression of the film. This shows again that the rhodamine-labelled polymer is much more line active due to its fluorescent label with the hydrophobic moiety. According to theory of hexagonal and stripe phases in monolayers, put forward by McConnell and co-workers,[47,48] the average width of an isolated stripe w_o is related to line tension λ as

$$w_0 = (2\varepsilon\delta)\exp(\lambda/\mu^2) \qquad (1)$$

where the factor $2e\delta$ represents the dipolar interactions, and μ is the dipole density difference between LE and LC phases. Hence the average width of stripes indicates a trade-off between the line tension and electrostatic repulsive forces. The stripes observed in the case of labelled polymer reflect an enormous reduction in the former, so that the latter dominates exclusively. Apparently, the fluorescent label, when added separately, is not sufficiently hydrophobic to accumulate at the domain boundary, and only the effect of the cholesterol anchor is visible. In contrast, the covalent attachment of the fluorescent moiety to the polymer through a hydrocarbon spacer locates the label at the interface and enables the probe to concentrate at the domain boundary.[49]

We also performed colocalization experiments of the polymer Ch-PEG$_{30}$-*b*-*hb*PG$_{17}$-Rho and a different lipid label, namely NBD-C$_{12}$-HPC. Due to the different absorbance and fluorescence wavelengths of the rhodamine label of the polymer and NBD connected to the lipid a two-channel excitation and emission experiment could be performed. The results clearly show that Ch-PEG$_{30}$-*b*-*hb*PG$_{17}$-Rho as well as NBD-C$_{12}$-HPC are located in the LE phase. As epi-fluorescence microscopy has limited resolution a clearly enhanced localization of the polymer at the domain boundaries could not be visualized. However, due to the lower fluorescence quantum yield of NBD, a higher concentration of NBD-C$_{12}$-HPC (0.2-0.8 mol%) was needed to obtain good images of the NBD-channel. This higher concentration influences the shape of the domains showing that NBD-C$_{12}$-HPC and the polymer compete for the domain boundaries (ESI† Fig. S4).

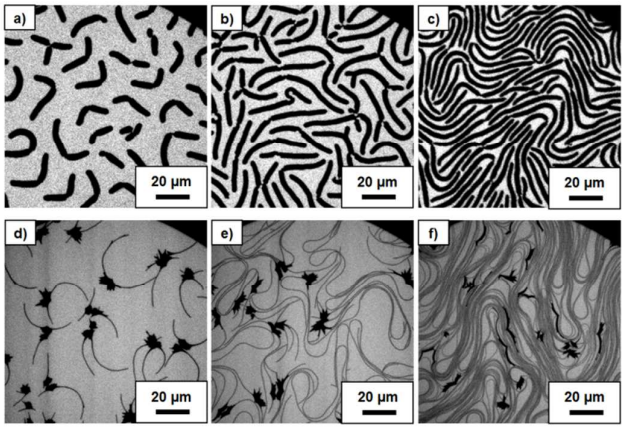

Fig. 4 Epi-fluorescence microscopy of monolayers of a)-c) rac-DPPC:Ch-PEG$_{30}$-*b*-*hb*PG$_{23}$ = 10:1 and d)-f) rac-DPPC:Ch-PEG$_{30}$-*b*-*hb*PG$_{17}$-Rho = 10:1 at surface pressures of a) 9.4 mN m^{-1}; b) 11.8 mN m^{-1}; c) 17.7 mN m^{-1}; d) 10.3 mN m^{-1}; e) 10.8 mN m^{-1}; f) 12.9 mN m^{-1}. Fluorescent dye: 0.01 mol% rhodamine-DHPE.

Time- and concentration-dependent adsorption measurements at the air/water interface

In order to test the polymers for their surface activity, concentration-dependent adsorption measurements of the polymers to the pure water surface were performed. After injection of different amounts of the polymer into the water subphase, the increase in surface pressure was recorded over a time period of 20 h (see Fig. 5a). Both polymers show a high surface activity. At the saturation concentration of ~9 µM for Ch-PEG$_{30}$-*b*-*hb*PG$_{23}$, the surface pressure was 28.6 mN m^{-1}. For Ch-PEG$_{30}$-*b*-*hb*PG$_{17}$-Rho the saturation concentration was somewhat lower with ~6 µM with a pressure of 27.3 mN m^{-1}. The results obtained with Ch-PEG$_{30}$-*b*-*hb*PG$_{23}$ are in agreement

with previous results of experiments using only one defined concentration of 2 µM.[26] The surface activity of Ch-PEG$_{30}$-*b*-*hb*PG$_{17}$-Rho is thus slightly higher compared to its non-labelled analogue, again probably caused by the amphiphilic fluorescent label. This is particularly evident when the surface pressure at a concentration of only 500 nM is compared, where the surface pressure values are 12 mN m^{-1} for Ch-PEG$_{30}$-*b*-*hb*PG$_{23}$ and 19 mN m^{-1} for Ch-PEG$_{30}$-*b*-*hb*PG$_{17}$-Rho.

Subsequently, we studied the adsorption of the polymers using the lowest concentration of only 500 nM to preformed L-DPPC and POPC monolayers, which were spread to distinct surface pressures (see Fig. 5b,c). The equilibrium surface pressure after injection of the polymers underneath the monolayer is reached after a significantly shorter time of only 2-3 h (not shown), i.e., the adsorption to the lipid monolayers occurs faster than to the air-water interface, indicating an additional driving force due to the presence of the lipid monolayer at the surface. A plot of $\Delta\pi$ vs. π yields the maximal insertion pressure MIP of a compound, when a linear fit of the data points is performed and extrapolated to $\Delta\pi = 0$. For this fit the first data points shown in Fig. 5b,c, representing the surface pressure of a pure polymer film at the same concentration, have to be excluded. The maximum insertion pressure of Ch-PEG$_{30}$-*b*-*hb*PG$_{23}$ adsorption to L-DPPC is more than ~44 mN m^{-1} and for Ch- PEG$_{30}$-*b*-*hb*PG$_{17}$-Rho adsorption to L-DPPC it is ~40 mN m^{-1}. For the adsorption to POPC monolayers the respective values are 39 and 44 mN m^{-1}.

The high MIP values are indicating a high insertion capability of both polymers into biological membranes, considering that the so-called monolayer-bilayer equivalence pressure is 30-35 mN m^{-1}.[34] Thus, both, the unlabelled and the rhodamine labelled polymer are capable of inserting into liquid expanded as well as into tightly packed liquid condensed PC monolayers, although only a very low amount of aqueous polymer solution was injected. Fig. 5b and c show that surface pressures reached after the adsorption of the polymers to phospholipid monolayers are considerably higher than the maximum surface pressures reached from adsorption of the polymers alone to the air-water interface. This leads to the conclusion that strong attractive forces between PCs and the used polymers Ch-PEG$_{30}$-*b*-*hb*PG$_{23}$ and Ch-PEG$_{30}$-*b*-*hb*PG$_{17}$-Rho exist. The polymer adsorption behaviour to phospholipid monolayers is different for both copolymers. Although they are both able to insert even into densely packed liquid condensed monolayers, the adsorption data for the rhodamine labelled polymer reveal higher surface pressure differences by adsorption than the unlabelled polymer. This difference is even more pronounced for adsorption to the liquid-expanded POPC monolayer. This agrees with the higher surface activity of the labelled polymer and is again caused by the additional amphipathic rhodamine label attached to the hyperbranched poly(glycerol) block.

The monolayer behaviour of zwitterionic lipids is not affected by the presence of sodium chloride or changes of the pH-value of the sub-phase between 2 and 8.[50,51] Aroti et al.[52] studied the effects produced by the ions of the Hofmeister series to phospholipid monolayers and concluded, "*Specific ion effects will be least noticeable on well-organised, flawless or rigid interfaces, where the entropy gain from their presence is minimal*". To investigate, if any of these factors have a bearing on the interactions of DPPC monolayers with the positively charged rhodamine moiety in the labelled polymer, additional measurements were carried out on 100 mM aqueous sodium chloride solution and phosphate buffer (pH 7.0) sub-phases. The maximum insertion pressures obtained from Fig. 5d are ~ 40 mN m^{-1} for all cases, indicating an insignificant effect of the sub-phase type.

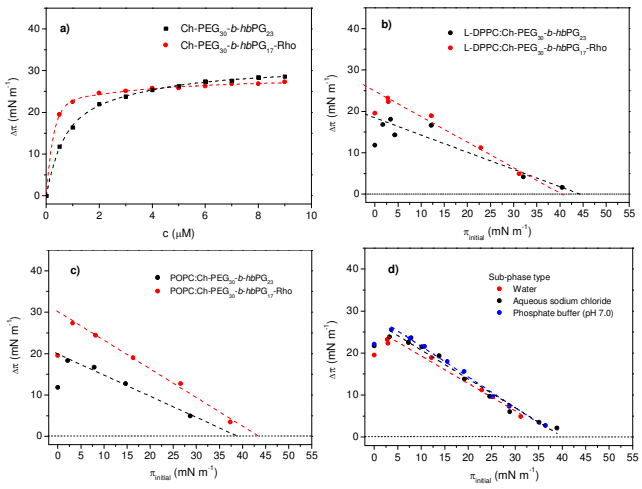

Fig. 5 a) Surface pressure as a function of concentration for the adsorption of the polymers to the pure air-water surface. b) Change in surface pressure $\Delta\pi$ observed for the adsorption to monolayers of L-DPPC with different initial surface pressure π c) Change in surface pressure $\Delta\pi$ observed for the adsorption to monolayers of L-POPC with different initial surface pressure π. Polymer concentration after injection was 500 nM in b) and c). d) Effect of sub-phase type on insertion of labelled polymer into L-DPPC monolayers.

Differential scanning calorimetry of lipid vesicles

In order to test, whether the different results obtained for the interaction of the two polymers with monolayers at the air-water interface are also observable with bilayer systems of the same phospholipids, differential scanning calorimetry (DSC) measurements were performed. DSC is a suitable tool to study the thermotropic behaviour of lipid bilayers. Changes in the width and temperature of the main phase transition of phospholipids from the gel to the liquid-crystalline lamellar phase are used as an indicator for the interaction of other molecules with the bilayer. For instance, the shift of the bilayer phase transition to lower temperatures with concomitant broadening of the transition is usually interpreted as an indication for the insertion of hydrophobic parts of the interacting molecule into the hydrophobic region of the bilayer.

The main phase transition temperature of pure DPPC vesicles occurs at 41.6 °C. After addition of different polymer concentrations to L-DPPC leading to molar ratios lipid:polymer of 100:1 to 5:1, the change of the main phase transition peak is investigated. For both polymers in mixtures with L-DPPC similar effects are observed. Only one major transition peak is

observed, demonstrating that no phase separation into large domains with different composition occurs. The transition peaks in Fig. 6a and b are shifted to lower transition temperatures with increasing amount of polymer. With higher mole fractions of the cholesterol-linked block copolymers the pre-transition of pure DPPC bilayers vanishes, which marks the transition from the ordered $L_{\beta'}$-phase to the $P_{\beta'}$-ripple phase. Also the sharp narrow DPPC main peak broadens and is almost absent for both 5:1 mixtures of L-DPPC with the polymers. The maximum in the shift is observed for the 5:1 mixture with a difference of 2.4 K for L-DPPC mixed with Ch-PEG_{30}-*b*-*hb*PG_{23} (see Fig. 6a) and of 2.2 K for L-DPPC mixed with Ch-PEG_{30}-*b*-*hb*PG_{17}-Rho (see Fig. 6b). The temperature downshift can be interpreted as a consequence of the incorporation of the cholesterol anchor into the bilayer membrane of DPPC. A molar ratio of 5:1 corresponds to 16.6 mol% of cholesterol incorporated into the bilayer. When the DSC curves in Fig. 6 are compared to those obtained with DPPC:cholesterol mixtures, similarities are observable. For instance, for cholesterol contents between 10 and 20 mol% in DPPC:cholesterol mixtures, the DSC peaks consist of a relatively sharp peak overlapping with an underlying broad peak, the sharper peak being shifted to lower temperatures compared to the main phase transition of pure DPPC.[1,2,5,15,54] This behaviour is quite similar to the peaks observed for DPPC mixed with Ch-PEG_{30}-*b*-*hb*PG_{23} shown in Fig. 6a, indicating that the major effect arises solely from the incorporation of the cholesterol moiety into the lipid bilayer. This is different for the polymer with the rhodamine label. The DSC curves in Figure 6b for high polymer contents do not show this superposition of the sharp component. While the cholesterol anchors the polymer to the lipid bilayer by incorporation into the hydrophobic region, the rhodamine label has again an influence on the bilayer system by eliminating the sharp peak caused by the transition of residual pure DPPC. The stronger interaction of the hyperbranched poly(glycerol) block with the attached amphipathic rhodamine label with the lipid headgroup region apparently leads to a better mixing of the system.

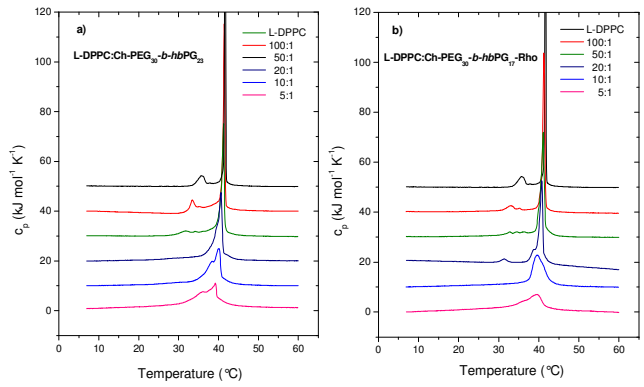

Fig. 6 DSC thermograms of the upscans of pure DPPC and the binary mixtures of L-DPPC:Ch-PEG_{30}-*b*-*hb*PG_{23} = x:1 (left) and L-DPPC:Ch-PEG_{30}-*b*-*hb*PG_{17}-Rho = x:1 (right).

Polymer interaction with giant unilamellar vesicles (GUVs)

Using confocal imaging, details of the interactions between the fluorescent labelled polymer in aqueous solution and GUVs of different phosphocholines can be studied. We find that the labelled block copolymer shows a high affinity to the different preformed GUVs of saturated 1,2-dilauroyl-*sn*-glycero-3-phosphocholine (DLPC), unsaturated 1,2-dioleoyl-*sn*-glycero-3-phosphocholine (DOPC) and mixed saturated/unsaturated 1-palmitoyl-2-oleoyl-*sn*-glycero-3-phosphocholine (POPC) (see Fig. 7 and 8). Fast polymer adsorption is already observed for a very small polymer/phospholipid ratio of 1/100, using a low polymer concentration of about 0.05 µM in aqueous solution. Quantitative analysis of the membrane fluorescence intensity is an indicator of polymer adsorption (ESI†, Fig. S3), i.e. it correlates with the polymer concentration (see Fig. 7a) and it is a function of time (see Fig. 7b). This clearly gives evidence for an interaction of the cholesterol anchor with the phospholipid membrane. The observed fluorescence intensity after insertion of the polymer into DLPC and DOPC GUVs was considerably higher than for insertion into POPC vesicles. Consequently, cholesterol is less attracted to POPC membranes compared to the DOPC- and DLPC-GUVs, despite the fact that all three lipids are in the liquid-crystalline state. The results from adsorption studies of the rhodamine-labelled

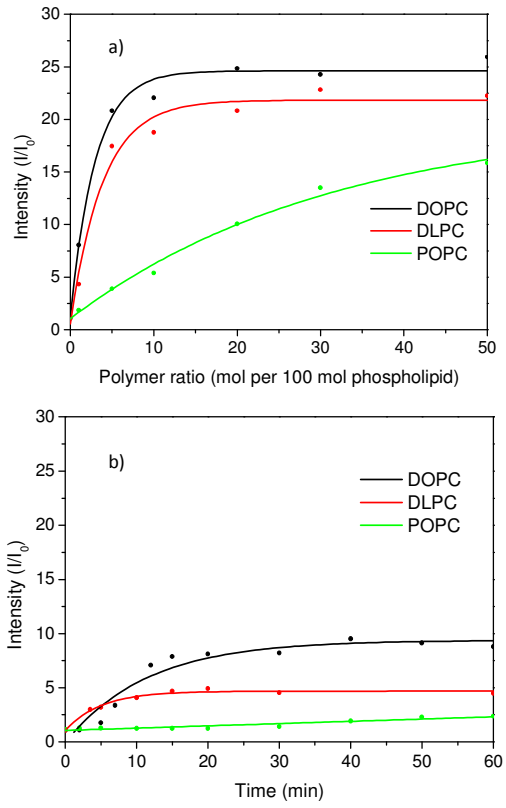

Fig. 7 Fluorescence intensity of Ch-PEG_{30}-*b*-*hb*PG_{17}-Rho at different single phase GUV membranes. a) Adsorption at different polymer ratios, data points taken at 30 min of incubation for the DLPC- and the DOPC-GUV, 1 h of incubation for the POPC-GUV; b) Time-dependent adsorption from Ch-PEG_{30}-*b*-*hb*PG_{17}-Rho/phospholipid molar ratio of 1/100.

polymer to phospholipid monolayers showed that only slight differences existed between adsorption to DPPC with saturated chains compared to POPC with one unsaturated chain. The differences in the insertion behaviour of the block copolymers into the lipid bilayer membranes are caused by differences in the cholesterol solubility in the hydrophobic regions of the bilayer systems.

Confocal images of the GUV equatorial layers, shown in Fig. 8, visualize the different insertion ability of the block copolymer into the membranes, decreasing in the order of DOPC>DLPC>POPC. Furthermore, the images show increasing rhodamine fluorescence intensity with increasing ratio of polymer addition, as analysed in Fig. 7a.

In addition, the rhodamine fluorescence distribution proves a homogeneous distribution of the polymer in the GUV membranes (see Fig. 8 and 9). Up to a polymer/phospholipid ratio of 20-30/100 the vesicles remain stable for several days and no significant desorption processes are observed by changing the polymer solution to pure water (see Fig. 9b). The addition of higher polymer concentrations affects the phospholipid membrane, the GUVs lose their stability and rigidity, and membrane fluctuations occur. Small membrane pieces are released inside and outside the bilayer, but nevertheless these GUVs remained stable for more than 24 h (see Fig. 9a). The observation of fluorescence from the polymer label inside the GUV may also indicate the capability of Ch-PEG$_{30}$-*b*-*hb*PG$_{17}$-Rho to generate membrane channels. Polymeric moieties might be able to cross the bilayer, and it is very likely that cholesterol is the anchor, which inserts into the outer as well as into the inner layer of the vesicular membrane. The more hydrophilic linear block as well as the hydrophilic hyperbranched block with the rhodamine label is exposed to water. Hence, the presented results match already published data on the interactions of cholesterol anchored poly(glycerols) with GUVs[33], as well as the more general knowledge about the membrane crossing properties of amphiphilic block copolymers depending on their molar mass and hydrophobic-hydrophilic balance. Tailored copolymers are thus able to insert and to span phospholipid membranes as well as to form and close bilayer pores.[25,26,55]

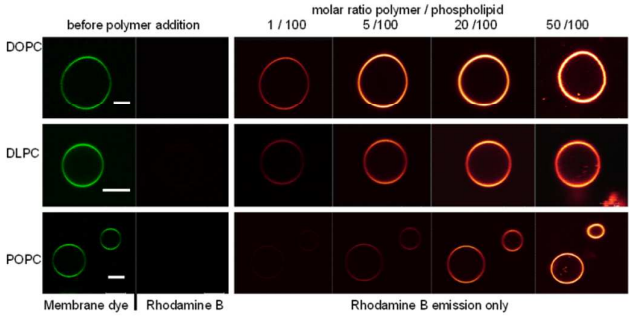

Fig. 8 Confocal images of DOPC, DLPC and POPC GUV vesicles after addition of polymer with increasing polymer/phospholipid ratio; green: membrane dye DiO; orange: rhodamine-labelled polymer Ch-PEG$_{30}$-*b*-*hb*PG$_{17}$-Rho. The scale bars represent 5 µm.

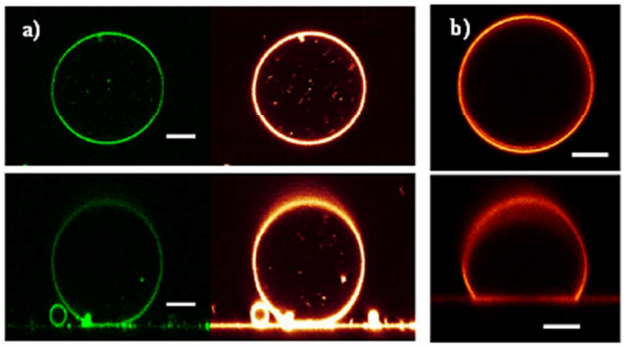

Fig. 9 Confocal images of immobilized DLPC GUVs before and after incubation in aqueous polymer solution; on top: equatorial single scans, below: vertical single scans; green: membrane dye DiO; orange: rhodamine-labelled polymer Ch-PEG$_{30}$-*b*-*hb*PG$_{17}$-Rho; a) 24 h incubation with polymer/phospholipid ratio of 1:2; b) GUV after polymer adsorption (1:10 polymer ratio) transferred to pure water for 2 h. The scale bars represent 5 µm.

Conclusions

In the present work, we investigated the interactions of the phospholipids DPPC and POPC with the synthetic polyphiles Ch-PEG$_{30}$-*b*-*hb*PG$_{23}$ and Ch-PEG$_{30}$-*b*-*hb*PG$_{17}$-Rho consisting of a cholesterol unit covalently linked to a hydrophilic polyether-based block copolymer. Both polymers differ in six glycerol units within the hydrophilic hyperbranched part, and a covalently linked rhodamine fluorescence label. Tensiometry showed a high surface activity for both polymers which is caused by the hydrophobic cholesterol moiety anchoring the polymer to the air/water interface. The labelled polymer, however, shows a higher surface activity than the unlabelled analogue, demonstrating that the linker and the rhodamine label apparently also possess amphipathic character and therefore increase the surface activity.

Monolayer experiments of mixed lipid/polymer systems showed the miscibility of both polymers with the phospholipid monolayers in co-spread films as well as in adsorption experiments using preformed lipid monolayers. Co-spreading experiments combined with epi-fluorescence microscopy showed for both polymer mixtures with DPPC new, and for both polymers very different, liquid-condensed domain shapes. The polymers are inserted into the lipid monolayer with the cholesterol moiety and accumulate at the LC domain boundaries, when the lipid film is compressed. Thus, the line tension between the LE and LC domains is reduced and new "interfaces" can now be formed more easily. This leads to a thinning of the LC domains, which can grow to very long stripes running parallel to each other and are not coalescing at higher pressure due to domain repulsion. An influence of the stereogenic centres of the cholesterol unit on the chirality of the LC domains was not observed. The rhodamine labelled

polymer was more effective in reducing the line tension. This is in line with its higher surface activity. Adsorption experiments confirmed the polymer insertion into phospholipid monolayers, even into LC layers of DPPC at high surface pressures. The observed MIP values were 40 mN m^{-1} or higher and thus well above the monolayer-bilayer equivalence pressure of 30-35 mN m^{-1}. Thus, the ability of the insertion of the polymers into model bilayer membranes was to be expected. This was indeed observed with lipid vesicle systems after addition of polymer. Increasing amounts of the block copolymer in the mixture with DPPC lead to significant changes in the thermotropic behaviour studied by DSC. The peak of the main transition of DPPC became much broader for lipid/polymer mixtures with molar ratios of 5:1. A comparison with the thermotropic behaviour of DPPC/cholesterol mixtures leads to the conclusion that indeed the polymers exhibit very similar effects on the transition behaviour due to their cholesterol anchor. However, the rhodamine labelled polymer exerts different effects due to the interaction of the rhodamine label with the lipid head group region. Additional experiments were performed with GUVs using CLSM. The GUV experiments again confirmed the high affinity of the polymers for phospholipid membranes. The results obtained with GUVs were in good agreement with adsorption measurements of the polymers to phospholipid monolayers. Quantitative analysis of the adsorption intensity of the rhodamine labelled polymer to different GUVs also confirmed the interaction of the cholesterol anchor with the phospholipid bilayers.

Acknowledgements

We thank the Deutsche Forschungsgemeinschaft (DFG) for financial support within the Forschergruppe FOR 1145 “Strukturbildung von synthetischen polyphilen Molekülen mit Lipidmembranen“ (TP 4, TP 3). S.S.M is a recipient of a fellowship through the Excellence Initiative (DFG/GSC 266). S.W.H.S is supported by a Ph.D scholarship from the Hazara University, Mansehra, Pakistan.

Notes and references

References

1 R. B. Gennis, *Biomembranes: Molecular structure and function*, 2nd edition. Springer-Verlag: New York, 2010.
2 A. Blume, P. Garidel, Lipid Model Membranes and Biomembranes (Chapter 3), in *From Macromolecules to Man,* R.B. Kemp, editor. Handbook of Thermal Analysis and Calorimetry Vol 4. Elsevier Press B.V.: Amsterdam 1999, 109 – 173.
3 G. W. Feigenson, *Biochim Biophys Acta*, 2009, **1788**, 47-52.
4 S. Bhattacharya, J. Biswas, *Langmuir*, 2010, **26**, 4642-4654.
5 J. R. Silvius, *Biochim. Biophys. Acta*, 2003, **1610**, 174-183.
6 Z. Chen, R. P. Rand, *Biophys. J.*, 1997, **73**, 267-276.
7 P. J. Quinn, C. Wolf, *Biochim Biophys Acta*, 2009, **1788**, 33-46.
8 V. Janout, S. Turkyilmaz, M. Wang, Y. Manaka, S. L. Regen, *Langmuir*, 2010, **26**, 5316-5318.
9 A. Radhakrishnan, H. M. McConnell, *Biochemistry*, 2000, **39**, 8119-8124.
10 W. C. Hung, W. T. Lee, F. Y. Chen, H. W. Huang,. *Biophys. J.*, 2007, **92**, 3960-3967.
11 R. A. Demel, L. L. M. Van Deenen, B. A. Pethica, *Biochim. Biophys. Acta*, 1967, **135**, 11-19.
12 H. Mozaffary, *Thin Solid Films*, 1994, **244**, 874-877.
13 S. K. Keller, A. Radhakrishnan, H. M. McConnell, *J. Phys. Chem. B*, 2000, **104**, 7522-7527.
14 A. Blume, *Biochemistry*, 1980, **19**, 4908-4913.
15 P. L. Chong, D. Choate, *Biophys. J.*, 1989, **55**, 551-556.
16 W. Kulig, J. Tynkkynen, M. Javanainen, M. Manna, T. Rog, I. Vattulainen, P. Jungwirth, *J. Mol. Model.*, 2014, **20**, 2121.
17 T. Rog, M. Pasenkiewicz-Gierula, K. M. Vattulainen I, *Biochim. Biophys. Acta Biomembr.*, 2009, **1**, 97-121.
18 M. Zocher, C. Zhang, S. G. F. Rasmussen, B. K. Kobilka, D. J. Muller, *Proc. Natl. Acad. Sci. USA*, 2012, **109**, E3463-E3472.
19 Y. Zhou, V. A. Briand, N. Sharma, S.-K. Ahn, R. M. Kasi, *Materials*, **2**, 2009, 636-660.
20 K. F. Rasmussen, A. A. A. Smith, P. Ruiz-Sachis, K. Edlund, A. N. Zelikin, *Macromol. Biosci.*, 2014, **14**, 33-44.
21 H. Ishiwata, A. Vertut-Doi, T. Hirose, K. Miyazima, *Chem. Pharm. Bull.*, 1995, **43**, 1005-1011.
22 Z.-P. Chen, L. Xiao, D. Liu, M.-S. Feng, Y.-Y. Xiao, J. Chen, W. Li, W.-D. Li, B.-C. Cai, *J. Appl. Polym. Sci.,* 2012, **124**, 4554-4563.
23 M. Tabbakhian, J. A. Rogers, *Res. Pharm. Sci.*, 2012, **7**, 43-50.
24 S. Reuter, A. M. Hofmann, K. Busse, H. Frey, J. Kressler, *Langmuir*, *2011*, **27**, 1978-1989.
25 E. Amado, J. Kressler, *Curr. Opin. Colloid Inter. Sci.*, 2011, **16**, 491-498.
26 X. Peng, A. M. Hofmann, S. Reuter, H. Frey, J. Kressler, *Colloid Polym. Sci.*, 2012, **290**, 579-588.
27 A. O. Fitton, J. Hill, D. E. Jane, R. Millar, *Synthesis-Stuttgart*, 1987, **12**, 1140-1142.
28 A. M. Hofmann, F. Wurm, E. Hühn, T. Nawroth, P. Langguth, H. Frey, *Biomacromolecules*, 2010, **11**, 568-574.
29 A. M. Hofmann, F. Wurm, H. Frey, *Macromolecules*, 2011, **44**, 4648-4657.
30 L. Zhao, S.-S. Feng, *J. Colloid Interface Sci.*, 2004, **274**, 55-68.
31 M. I. Angelova, D. S. Dimitrov, *Faraday Discuss. Chem. Soc.*, 1986, **81**, 303-311.
32 B. Lohse, P. Y. Bolinger, D. Stamou, *J. Am. Chem. Soc.*, 2008, **130**, 14372-14373.
33 R. Schöps, E. Amado, S. S. Müller, H. Frey, J. Kressler, *Faraday Discuss. Chem. Soc.*, 2013,**166**, 303-315.
34 A. Blume, *Biochim.Biophys.Acta*, 1979, **557**, 32-44.
35 M. Winterhalter, H. Bürner, S. Marzinka, R. Benz, J. J. Kasianowicz, *Biophys. J.*, 1995, **69**, 1372-1381.
36 T. L. Kuhl, J. Majewski, P. B. Howes, K. Kjaer, A von Nahmen, K. Y. C. Lee, B. Ocko, J. N. Israelachvili, G. S. Smith, *J. Am. Chem. Soc.*, 1999, **121**, 7682-7688.
37 F. Müller-Landau, D. A. Cadenhead, *Chem. Phys. Lipids*, 1979, **25**, 299-314.
38 T. R. Baekmark, G. Elender, D. D. Lasic, E. Sackmann, *Langmuir*, 1995, **11**, 3975-3987.
39 V. Tsukanova, C. Salesse, *Macromolecules*, 2003, **36**, 7227-7235.
40 V. Tsukanova, C. Salesse, *J. Phys. Chem. B*, 2004, **108**, 10754-10764.
41 A. Hädicke, A. Blume, *J. Coll. Interf. Sci.*, 2013, **407**, 327-338.
42 H. M. McConnell, *Annu. Rev. Phys. Chem.* 1991, **42**, 171-195.
43 P. Krüger, M. Lösche, *Phys. Rev. E*, 2000, **62**, 7031-7043.
44 P. Scholtysek, Z. Li, J. Kressler, A. Blume, *Langmuir*, 2012, **28**, 15651-15662.
45 R. M. Weis, H. M. McConnell, *J. Phys. Chem.*, 1985, **89**, 4435-4459.

46 D. J. Keller, H. M. McConnell, V. T. Moy, *J. Phys. Chem.*, 1986, **90**, 2311-2315.
47 H. M. McConnell, V.T. Moy, *J Phys. Chem*., 1988, **92**, 4520-4525.
48 H. M. McConnell, *Proc. Natl. Acad. Sci*., 1989, **86**, 3452-3455.
49 A. A. Bischof, A. Mangiarotti, N. Wilke, *Soft Matter*, 2015, **11**, 2147-2156.
50 D.O. Shah, J. H. Schulman, *J. Lipid Res*., 1965, **6**, 341-349.
51 V. L. Shapovalov, *Thin Solid Films*, 1998, **327-329**, 599-602
52 A. Aroti, E. Leontidis, E. Maltseva, G. Brezesinski, *J. Phys. Chem. B*, 2004, **108**, 15238-15245.
53 R. M. Weis, *Chem. Phys. Lipids*, 1991, **57**, 227-239.
54 T.-H. Huang, C.W.B. Lee, S. K. Das Gupta, A. Blume, R.G. Griffin, *Biochemistry*, 1993, **32**, 13277-13287.
55 E. Amado, A. Blume, J. Kressler, *React. Funct. Polym.***,** 2009, **69**, 450-456**.**

Graphical Abstract

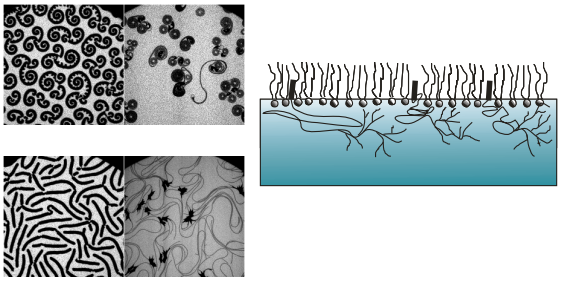

Interactions of phospholipid membranes with novel linear-hyperbranched block copolymers with a cholesterol anchor are studied.